A Probabilistic Approach of Space Objects Detection from Non-resolved Optical Observation

XIAO BIAN
NORTH CAROLINA STATE UNIVERSITY
BROOKE N. GIBSON
OCEANIT, Inc.
HAMID KRIM
NORTH CAROLINA STATE UNIVERSITY

ABSTRACT

Non-resolved optical space imagery is usually heavily noisy with many field stars clutter. Both phenomena may impair the success of detecting space objects. There is hence often a need for efficient and robust preprocessing techniques to filter the objects of interest.

In this paper, we propose a novel probabilistic approach for denoising, filtering and detecting space objects by using non-resolved optical images. In particular, as pixels of background and foreground in an image obey different probabilistic distributions, we propose a corresponding clustering algorithm to distinguish foreground objects from background noises. Furthermore, a near real-time finer classification for foreground objects is achieved by further exploring the metric on the filtered pixel set. Various modes (sidereal tracking/stationary) and different types of objects (GEO/LEO) are unified into this general framework. We verify the effectiveness and robustness of our algorithm by detecting and filtering space objects in CCD telescopic sequential imageries under different experimental conditions.

1. INTRODUCTION

Non-resolved optical observation of space targets plays a key role on space debris analysis [1][2][3] and LEO/GEO satellites characterization [4][5][7] for its important photometric information as well as the cost-effective system. It is widely used in the detection of unidentified space debris/objects, and moreover, the light curve of a target can then be extracted to estimate physical characteristics of the space object. Nevertheless, non-resolved optical images often have low SNR as well as field stars as clutters, and hence lead to heavy preprocesses to denoise, detect and identify the target of interest in current techniques [3]. The high computational cost impact the potential of related algorithms for important near real-time detection.

From another perspective, most of the denoising techniques in the area of image processing are also problematic when directly applying to telescopic imagery. First of all, the traditional filter-based methods, relied on the sharp difference between distributions of noise component and the true signal, are not good at the situation when noise terms are both dense and with high energy. On the other hand, more recent techniques based on sparse modeling [6], although have the advantage to preserve the texture information, have formidable computational cost and hence are difficult to applied to near real-time applications.

In this paper, we proposed a novel method specifically for telescopic imagery processing. We build a probabilistic model for pixel values in the image domain, upon which local statistics of each point is used to classify foreground objects from background. Furthermore, a corresponding clustering method is designed to classify different objects by exploiting a proper metric space for foreground pixels. The rest of the paper is organized as follows. In Section 2, the probabilistic model for pixel values in telescopic imagery is presented with the associated hypothesis test to distinguish foreground/background pixels. In Section 3, we illustrate the metric space of foreground pixels and describe the algorithm to classify and label points in different objects. In Section 4, we show the experimental results of non-resolved optical imagery filtering and detection on telescopic images of space objects. Finally, Section 5 concludes this paper.

2. A PROBALISTIC MODEL FOR PIXELS IN TELESCOPIC IMAGES

Different from natural images, the distribution of pixels in non-resolved optical imagery has some distinctive properties. First of all, only very few pixels have true values other than zero. For a typical non-resolved imagery, as Fig. 1, merely less than 3% percent of the total pixels are for targets or stars. The rest of them are all from background. The low percentage of meaningful signals practically makes learning algorithms from data problematic. Second, all pixels are contaminated by heavy Gaussian noises, especially for the ones with lower true intensity or belong to the background. We can see the distribution of pixel values from the histogram in Fig. 2 very close to a Gaussian distribution.

These features lead us to the idea of classification-based denoising of telescopic images. Instead of filtering noise component for every pixel in image domain, it would be more efficient to exclude all background pixels and identify the pixels that matter. We therefore present a probabilistic framework for the task of classification-based denoising and filtering in this section.

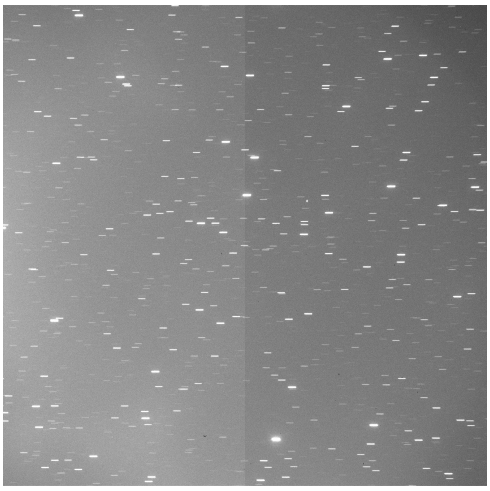

Fig. 1. A typical non-resolved telescopic image

Specifically, for any pixel in the telescopic image domain, it follows an underlying probabilistic model:

$$I(T) = i_T + n,\ n \sim G(\mu_T, \sigma_T),$$

where T is the label for the object which the pixel belong to.

Based on this probabilistic model, hypothesis test can be directly applied to identifying if a pixel belongs to a certain object. However, strong Gaussian noises can severely deteriorate the performance of the test. We hence further consider the spatial relations among pixels to enhance the results.

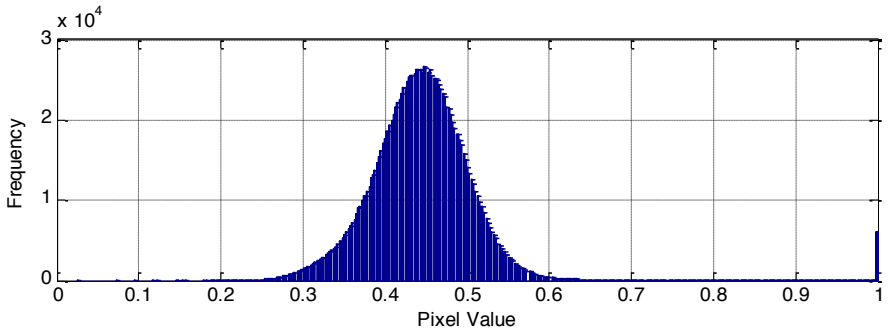

Fig. 2. The histogram of pixel values in Fig. 1

In specific, points in the image domain are partitioned into three parts in regard to the statistics of their neighborhood: background set *W*, interior set *S* and boundary set *B*. The three sets correspond to the background, the inner part of objects and the boundaries between each object and the background, respectively. The strict definitions are given as follows:

Definition 1 (Background Set) For points in the image domain, the set of all background points is

$$W = \left\{ p \in W \mid \forall q \in N(p), f(p) = f(q) = G\left(\mu_0, \sigma_0^2\right) \right\},$$

where *f* is the probability density function, and *N(p)* is the neighborhood of point *p*.

Definition 2 (Interior Set) For points in the image domain, the set of all interior points (in regard to objects) is

$$S = \left\{ p \in S \mid \forall q \in N(p), f(p) = f(q) \neq G\left(\mu_0, \sigma_0^2\right) \right\},$$

where *f* is the probability density function, and *N(p)* is the neighborhood of point *p*.

Definition 3 (Boundary Set) For points in the image domain, the set of all boundary points is

$$B = \left\{ p \in B \mid \exists q \in N(p), f(p) \neq f(q), f(p) \neq G\left(\mu_0, \sigma_0^2\right) \right\},$$

where *f* is the probability density function, and *N(p)* is the neighborhood of point *p*.

Intuitively, the statistically homogeneous part of one image is extracted and then divided into interior set and background set. When the neighborhood of some points does not hold such homogeneity, we treat them as boundary points of the above two sets.

Based on the above definitions, we can do a hypothesis test to find the interior set of a given image. Specifically, let $f_0 = G(\mu_0, \sigma_0)$ be the distribution of background pixels, and $f_p = G(\mu_p, \sigma_p)$ be the distribution of object pixels with $\mu_p > \mu_0$, we have

$$H_0 : p \sim f_p, q \sim f_p, \forall q \in N(p)$$
$$H_1 : f_p \neq f_0 \text{ or } f_p \neq f_q, \forall q \in N(p)$$

With the label of pixels achieved by the hypothesis test, we filter out the background of the image and only keep the pixels from each object. In Fig. 3, we show the labels of interior set of a telescopic image and simply set the background to be black. Since the background usually does not have the information of the target of interest, it is unnecessary to process the background part. Therefore the following analysis can focus on this small subset of points in the image domain.

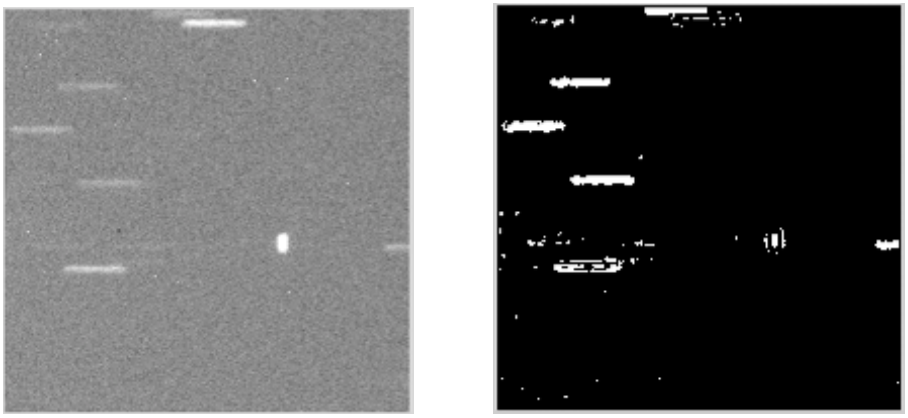

(a) The original image (b) the interior set of (a)

Fig. 3. An example of finding interior set (white pixels in (b) means the ones in the interior set)

It is worth noting that the statistics of the value of background pixels can be estimated from the given image itself. In Fig. 2, we show that the distribution of pixel values for a typical telescopic image resembles Gaussian distribution, and in most cases, more than 97% of the pixels are in the background set. Therefore the estimation can simply use all the pixels except the top 3% bright ones.

3. INTERIOR POINTS CLUSTERING

With the foreground pixels classified from the background, we extract high-level information about objects from the set of points. The crucial step next would be to identify the label of each point with respect to objects, to which a proper distance measure is important. Ideally, this distance measure should reflect both the physical properties, such as the apparent magnitude, as well as the spatial relations.

We hence define a metric on the S as follows,

$$\begin{aligned} &\forall p_a, p_b \in S, \\ &d\left(p_a, p_b\right) = d_{Eucidean}\left(p_a, p_b\right) + d_{Intensity}\left(p_a, p_b\right) \\ &\qquad = \sqrt{\left(p_a^x - p_b^x\right)^2 + \left(p_a^y - p_b^y\right)^2} + \beta\left|I\left(P_a\right) - I\left(P_b\right)\right|, \end{aligned}$$

where β is a weighted parameter to balance between the intensity distance and the Euclidean distance in the image domain.

Intuitively, we map a smaller distance to the points that both share similar intensity and are close to each other, and a larger one vice versa. The distance matrix hence is then used as an input to a clustering algorithm. In this paper, we utilize the single linkage clustering for grouping points together. In specific, two sets of points A and B are considered to be from the same cluster if and only if

$$\min\left\{d\left(p_a, p_b\right) : p_a \in A, p_b \in B\right\} < \gamma .$$

This method has the advantage of low computational cost compared to other clustering method, like hierarchical clustering, and does not need the number of clusters as the prior information as K-means. The cut-off distance γ can be estimated from sample images. Concretely, it is determined by the size of objects in the image domain.

Since the metric defined above is determined by three parameters: x, y and $I(p)$, we are able to embed the points in a 3-dimensional space and preserve the metric. The results are shown in Fig. 4. We can see the points are clearly clustered together according to their labels.

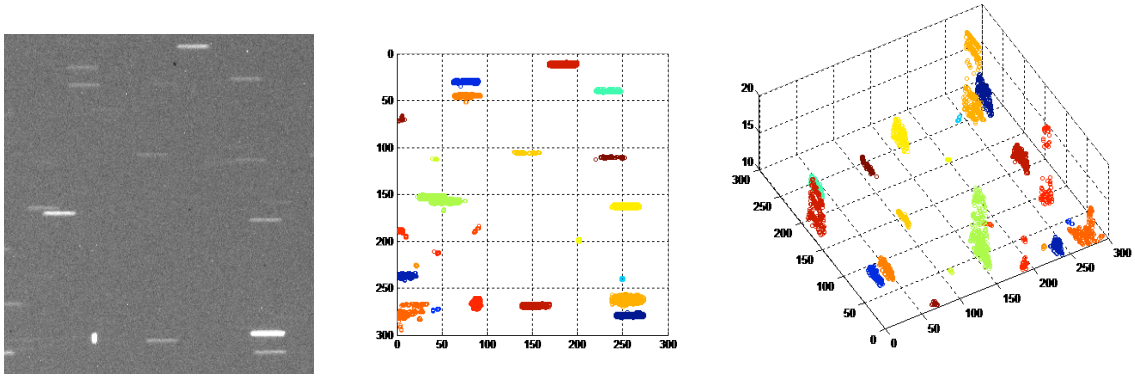

(a) The original frame (b) Points in the metric space (c) Points in the metric space from a different angle

Fig. 4. The clustering results (Different color means different objects identified)

After retrieving the object-level information from the image, physical features of each object can be used to classify objects and to further identify the target of interest. Due to different trajectories and the effect of exposure time, the spatial distribution for various types of objects behaves quite different. Here we show two fundamental scenarios, the stationary mode and the sidereal mode, in Fig. 5. For the stationary mode, the telescope is relatively stationary to the earth. Since the rotation of earth contributes the relative motion of stars to earth, which also affect telescope in this scenario, we will observe stars like streaks in the image domain due to the exposure time. On the contrary, when the telescope runs in the sidereal tracking mode, stars are relatively stationary, and any object having a different motion to stars will show as a streak. The length of the streak is determined by both the exposure time and the motion of the target.

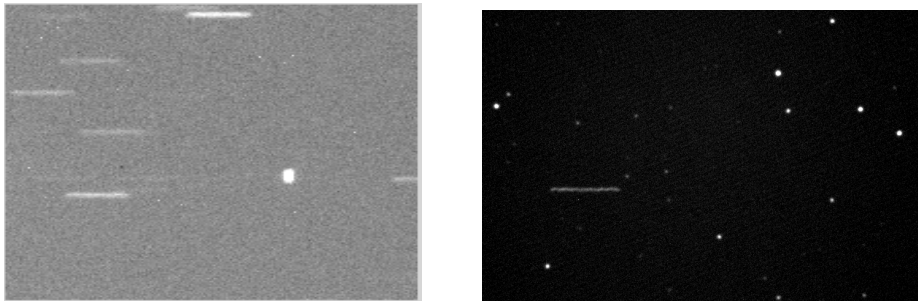

(a) Stationary mode (b) Sidereal tracking mode

Fig. 5. Sample images of the two scenarios (In (a), a GEO object is shown as a white dot. In (b), a LEO object is shown as a streak.)

In both scenarios, we use the ratio of width and height of an object in the image domain as one unified criterion to identify targets from stars. Specifically, let X be a set of pixels representing an object, and the spread of its pixels defined as $R(X) = W/H$, then X is a target of interest if

$$\left|R(X) - c\right| > median\{R\},$$

where c is the parameter measured the distance between a target of interest and stars, and $median\{R\}$ is the median of width-height ration for all objects.

Intuitively, this criterion can be seen as a simple way to pick the outliers. Since in one image most of the bright objects would be stars, the target of interest is expected to have different motion patterns.

4. EXPERIMENTAL RESULTS

In this section, we show the experimental results of our processing method for non-resolved optical images on telescopic image sequences.

The computational cost of our method is mainly composed of two parts: 1) the computational cost for hypothesis test; 2) the computational cost to extract object-level information and detection. In specific, the computational cost of hypothesis test is $O(nd^2)$, where n is the number of pixels, and d is the size of neighborhood for statistical analysis. In our experiments, $d = 9$ is sufficient to provide reasonably good results, and therefore the computational cost in this step is linear to n. For the latter one, the computational complexity is $O(m^2)$, where m is the size of interior set. It is worth noting that m is only 2%~3% of the total pixels in a typical non-resolved optical image, which results in a similar computational cost compared to the first step in most cases.

In Fig. 6, a space target is detected and filtered from the original low SNR images in the sidereal tracking mode. Specifically, three sequences under different exposure time (8s, 2s and 1s) are processed here. A shorter exposure time usually lead to harder detection, since the difference of motions would not be as significant, and also the SNR of the image would be lower. In these experiments, we show the successful detection and identification in all conditions of a space target.

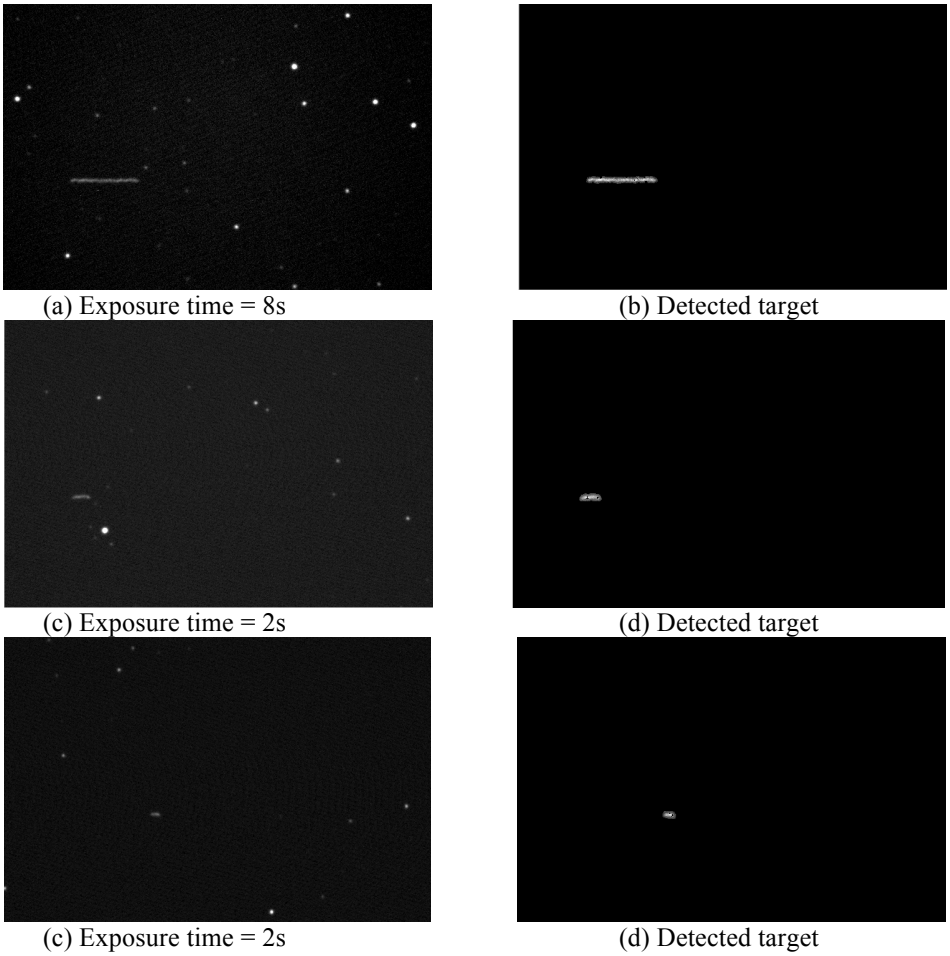

(a) Exposure time = 8s (b) Detected target

(c) Exposure time = 2s (d) Detected target

(c) Exposure time = 2s (d) Detected target

Fig. 6. Processed results for sidereal tracking mode with different exposure time

In Fig. 7, we show the processed results of another telescopic image sequence under the stationary mode. All the stars in the image domain show as streaks, and for GEO objects, since they are relative stationary to the earth, they appear like dots in the image domain. In the experiments, we show that the stars and noise components are removed, and only the target of interest is preserved.

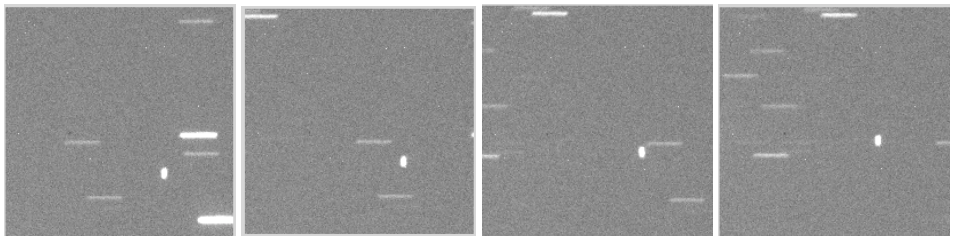

(a) The raw image sequence

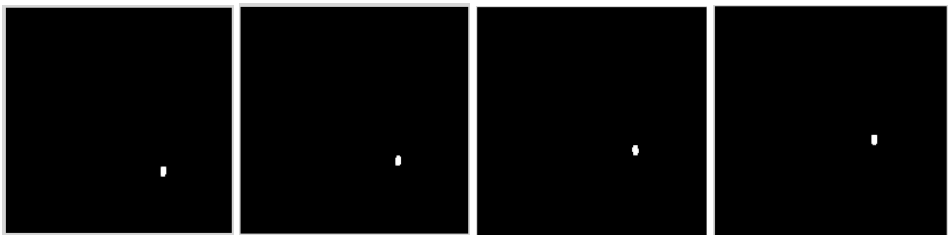

(b) The processed image sequence

Fig. 7. Processed results of a GEO object images sequence

5. CONCLUSION

In this paper, we have presented a novel method for non-resolved optical image processing. Local statistics are exploited to build an interior set of pixels for distinguishing space objects from noise components. Furthermore, clustering-based method extracts object-level information from pixel-level statistics. We apply this method to image sequences on both sidereal tracking mode and the stationary mode. The successful detection of GEO targets in two fundamental scenarios validates the effectiveness of our method.

Future works may include the integration of temporal information among frames in an image sequence. The correlations among frames may be helpful to target detection. Also it would be interesting to see further experiments on the detection rate of LEO/GEO targets on larger dataset.

6. ACKNOWLEDGEMENT

We would like to express our gratitude to MDA to support this project. We also would like to appreciate the assistance on collecting data and helpful comments from OCEANIT and Czech Technical University in Prague.

7. REFERENCES

1. Duncan, R.B. et al, High Resolution Near Real Time Image Processing and Support for MSSS Modernization, AMOS, 2012
2. Seitzer, P. et al, Visible Light Spectroscopy of GEO Debris, AMOS, 2012
3. Yanagisawa, T et al, Comparison between Four Detection Algorithms for GEO Objects, AMOS, 2012
4. 1 J. Murray-Krezan, S. A. Gregory, W. C. Inbody, A. Dentamaro, and P. Dao, “Automated Characterization of Three-Axis Stabilized GEOs Using Non-Resolved Optical Observations,” MIT LL Space Control Conference, 2012.

5. A. B. Chaudhary, T. Payne, S. A. Gregory, and P. Dao, Fingerprinting of Non-resolved Three-axis Stabilized Space Objects Using a Two-Facet Analytical Model, AMOS Tech Conference 2011.
6. Michael Elad and Michael Aharon, Image Denoising via Sparse and Redundant Representations with Learned Statistical Dependencies. In Acoustics, Speech and Signal Processing (ICASSP), 2011 IEEE International Conference on, Page 5820 – 5823.
7. James Frith, Brooke Gibson, Russell Knox, Kawailehua Kuluhiwa, Simultaneous Single Site Color Photometry of LEO Satellites, AMOS 2008